04,06

Effect of acceptor doping on the dielectric properties of sodium niobate ceramics

© E.V. Barabanova, N.M. Ospelnikov, A.I. Ivanova, A.Yu. Karpenkov

Federal State Budgetary Educational Institution of Higher Education „Tver State University“, Tver, Russia

E-mail: pechenkin_kat@mail.ru

Received December 13, 2024
Revised April 3, 2025
Accepted April 7, 2025

The search for new functional materials is inextricably linked with modification of the properties of already known materials with optimal parameters. Thus, sodium niobate is used as a basis for complex lead-free ferroelectric oxides. This work is devoted to the study of the structure and dielectric properties of sodium niobate ceramics doped with Bi and Fe in concentrations of 10, 20 and 30 mol.%, in a wide range of frequencies ($1-10^6$ Hz) and temperatures ($30-650\,^\circ$C). It was found that with an increase in the impurity concentration, the average grain size decreases from $5-10\,\mu$m to $0.5-2\,\mu$m, the heterogeneity of the microstructure increases, and the grain shape becomes closer to cubic. At the same time, the volume of the unit cell increases with an unchanged symmetry of the crystal lattice ($Pmc2_1$). The method of dielectric spectroscopy revealed the presence of two relaxation processes corresponding to ionic thermal polarization and conductivity relaxation, which affects the temperature dependence of the permittivity. The doping leads to an increase in the temperature region of phase transitions and a shift of T_m by approximately $150\,^\circ$C to lower temperatures.

Keywords: sodium niobate, heterovalent doping, perovskite structure, electrical conductivity, diffuse phase transition.

DOI: 10.61011/PSS.2025.04.61264.342

1. Introduction

Sodium niobate $NaNbO_3$ (NN) has been of undying interest to researchers around the world for decades. It is a convenient material for creating solid solutions based on it, possessing ferroelectric properties, which are considered as possible substitutes for lead-containing lead zirconate-titanate (PZT) ceramics. Despite the large number of experimental data, there is no consensus in the scientific literature on the pattern of phase transitions in sodium niobate, its ferroelectric properties, electrical conductivity, etc. Initially, sodium niobate at room temperature was considered as an antiferroelectric (P phase). A total of 6 phase transitions were found in it: U (paraelectric, $Pm\bar{3}m$) $\rightarrow 913\,\mathrm{K} \rightarrow T_2$ (paraelectric, $P4/mbm$) $\rightarrow 848\,\mathrm{K} \rightarrow T_1$ (paraelectric, $Cmcm$) $\rightarrow 793\,\mathrm{K} \rightarrow S$ (paraelectric, $Pmmn$) $\rightarrow 753\,\mathrm{K} \rightarrow R$ (antiferroelectric, $Pmmn$) $\rightarrow 633\,\mathrm{K} \rightarrow P$ (antiferroelectric, $Pbcm$) $\rightarrow 173\,\mathrm{K} \rightarrow N$ (ferroelectric, $R3c$) [1]. But on closer study, it was found that it can also exhibit ferroelectric properties at room temperature (Q phase, $Pmc2_1$) when an external electric field, pressure is applied or when doped [2–5]. There is also evidence for the existence of three other phases within the P phase: monoclinic ($250-410\,\mathrm{K}$), incommensurate ($410-460\,\mathrm{K}$), and orthorhombic ($460-633\,\mathrm{K}$) [6]. In some papers it is noted that when the grain size of ceramics decreases below $0.27\,\mu$m, Q phase [7,8] stabilizes, but the presence of defects such as oxygen vacancies leads to the stabilization of phase P [9].

In order to obtain NN-based materials with application-specific properties, various kinds of compositional modifications are carried out, for example, by introducing impurities. The substitution of metal ions both at A-site and at B-site is possible during synthesis according to the general formula of the class of perovskite-type compounds (ABO_3) to which sodium niobate belongs. The valences of the main and impurity ions must be taken into account. Thus in alkali metal niobates, particularly and NN, the valence of the ion A is $+1$, and that of the ion B is $+5$. A substitutional impurity can be either isovalent (with the same valence values) or heterovalent, with the most common case being donor-type at the A-site and acceptor-type at the B-site. In this case, various kinds of defects are formed in the NN crystal lattice according to the condition of electroneutrality of materials. The type of defect is determined by the type of impurity. For example, acceptor doping at B-site results in a decrease in the total positive charge. Therefore, vacancies in the anionic sublattice, i. e., oxygen vacancies, are simultaneously formed in the material to maintain the electroneutrality of the material. The deficiency of cations, which is formed during the synthesis of ceramics due to the high volatility of alkali metal compounds, also leads to similar defects. The presence of vacancies in the crystal lattice is an important condition for the existence of ionic conduction in solids. Therefore, a number of studies consider sodium niobate with various kinds of point defects and dopants as a

promising solid-state electrolyte [10]. Other authors note its semiconductor properties [11] or consider it as a material for energy storage devices [12,13]. In connection with all of the above, it is relevant to continue studies of changes in the physical properties of sodium niobate depending on the type and concentration of the dopants.

Sodium niobate ceramics doped with iron and bismuth are considered in the proposed study. Substitution of Nb^{5+} occurs at *B*-site by Bi^{3+} and Fe^{3+} in equal concentrations according to the formula $Na(Fe_{0.5}Bi_{0.5})_xNb_{1-x}O_{3-\delta}$, at $x = 0.1$ ($NN_{0.9}FB$), $x = 0.2$ ($NN_{0.8}FB$), $x = 0.3$ ($NN_{0.7}FB$), where δ is some concentration of oxygen vacancies. The effect of impurity concentration on the structure and dielectric properties of the material is studied.

2. Methodology

The samples were fabricated according to conventional ceramic technology by a two-step method. The following chemical reagents were used as the initial components according to the above chemical formulas: sodium carbonate (Na_2CO_3), niobium (V) oxide (Nb_2O_5), iron (III) oxide (Fe_2O_3), and bismuth (III) oxide (Bi_2O_3). The raw materials were thoroughly mixed using mortar and pestle in ethyl alcohol medium. The pre-compressed mixtures were synthesized at 700 °C for 4 hours in corundum crucibles in an air atmosphere. After regrinding, the powders were pressed at 650 MPa into pellets with a diameter of 10 mm by cold one-sided pressing in a metal mold. The samples were then sintered at 1100 °C ($NN_{0.9}FB$ and $NN_{0.8}FB$) and 1000 °C ($NN_{0.7}FB$) for 4 hours. Silver-containing paste was applied to opposite surfaces of the samples and annealed at 450 °C to create electrodes.

The dielectric properties were studied by dielectric spectroscopy. For this purpose, capacitance and dielectric loss angle tangent were measured using a Frequency Response Analyzers PSM1735 with Impedance Analysis Interface (Newtons4th Ltd) in the frequency range $1-10^6$ Hz and in the temperature range from room temperature to 650 °C in steps of 10 °C. The heating rate did not exceed 1.5 °C/min.

Electron microscopic studies of the microstructure were performed using JEOL JSM-6610LV scanning electron microscope. Sample preparation consisted of sputtering a conductive layer of Pt. The secondary electron imaging (SEI) was used to determine the sample topography.

The phase composition of the ceramic samples was determined using X-ray diffractometer „DRON-7". An X-ray tube with Cu$K\alpha$-radiation ($\lambda = 0.1540598$ nm) was used as the x-ray source. The unit cell parameters were determined from the reflexes corresponding to reflections from a series of planes (*hkl*) in the region of angles $2\theta = 15-105°$. The ceramic sample was ground in an agate mortar to a grain size smaller than 10 μm, sieved through sieves with a given grain size, mixed with a diluent (petroleum jelly), and placed in a well (1 mm deep) of a quartz cuvette. The excess sample was cut off in one touch with the edge of the glass plate. This technique avoided the appearance of undesirable texture along the cleavage planes or crystallite facet, which is a nuisance when measuring the position of the peaks in the diffraction pattern.

3. Results

Untreated samples without electrodes were chosen to study the surface morphology. As can be seen in Figure 1, the $NN_{0.9}FB$ sample has grains shaped like polyhedrons. Their average size is $5-10\,\mu$m. A high packing density of grains is observed and pores are almost absent. The grain growth steps are clearly visible. This structure is characteristic of industrially important PZT ceramics and barium titanate [14]. It is characterized by the presence of triple junction points (neighboring grain boundaries join at an angle of 120°) and hexagonal grains (in plane), which is characteristic of a thermodynamically equilibrium structure.

The grains are also polyhedrons in the $NN_{0.8}FB$ sample, but with more right angles, which increases the porosity of the sample. The grain size distribution is inhomogeneous, but it can be noted that small grains prevail, with an average size of $2-7\,\mu$m. $NN_{0.7}FB$ sample has a finely dispersed structure with an average grain size of $0.5-2\,\mu$m, the growth steps are indistinguishable, and the grain shape is close to cubic. Thus, a decrease in niobium concentration leads to a decrease in grain size, a change in grain shape and an increase in porosity (Figure 1). The result is consistent with literature data, since the decrease in ceramic grain size with increasing acceptor dopant concentration has been reported by a number of researchers [10,15].

X-ray diffraction analysis was performed to determine the crystal structure of the ceramics. According to the obtained data, the unit cell of NNFB ceramics for all three compositions corresponds to the distorted perovskite cell — orthorhombic modification of perovskite structure with space group $Pmc2_1$ (Figure 1, *b, d, f*). This is consistent with the literature data for sodium niobate [16]. As the results show, as the niobium concentration decreases, the unit cell shrinks along the *c* axis (by 0.42 %) and expands along the axes *a* and *b* (by 0.43 and 0.36 %, respectively). Moreover, the decrease of the niobium concentration and increase of the acceptor dopant concentration lead to an increase in the number of defects in the ceramic structure, in particular oxygen vacancies. Thus, it can be concluded that as the number of oxygen vacancies increases, the volume of the crystal cell increases without changing the lattice symmetry. This agrees well with the literature data [11].

At the same time a minor presence of the second phase is observed in the sample with 70 % niobium concentrations, which could not be identified. That is, samples with niobium concentrations above 80 mol.% are single-phase solid solutions, and samples with lower niobium concentrations are composites. Thus, the impurity solubility limit for sodium niobate doped simultaneously with iron and bismuth at

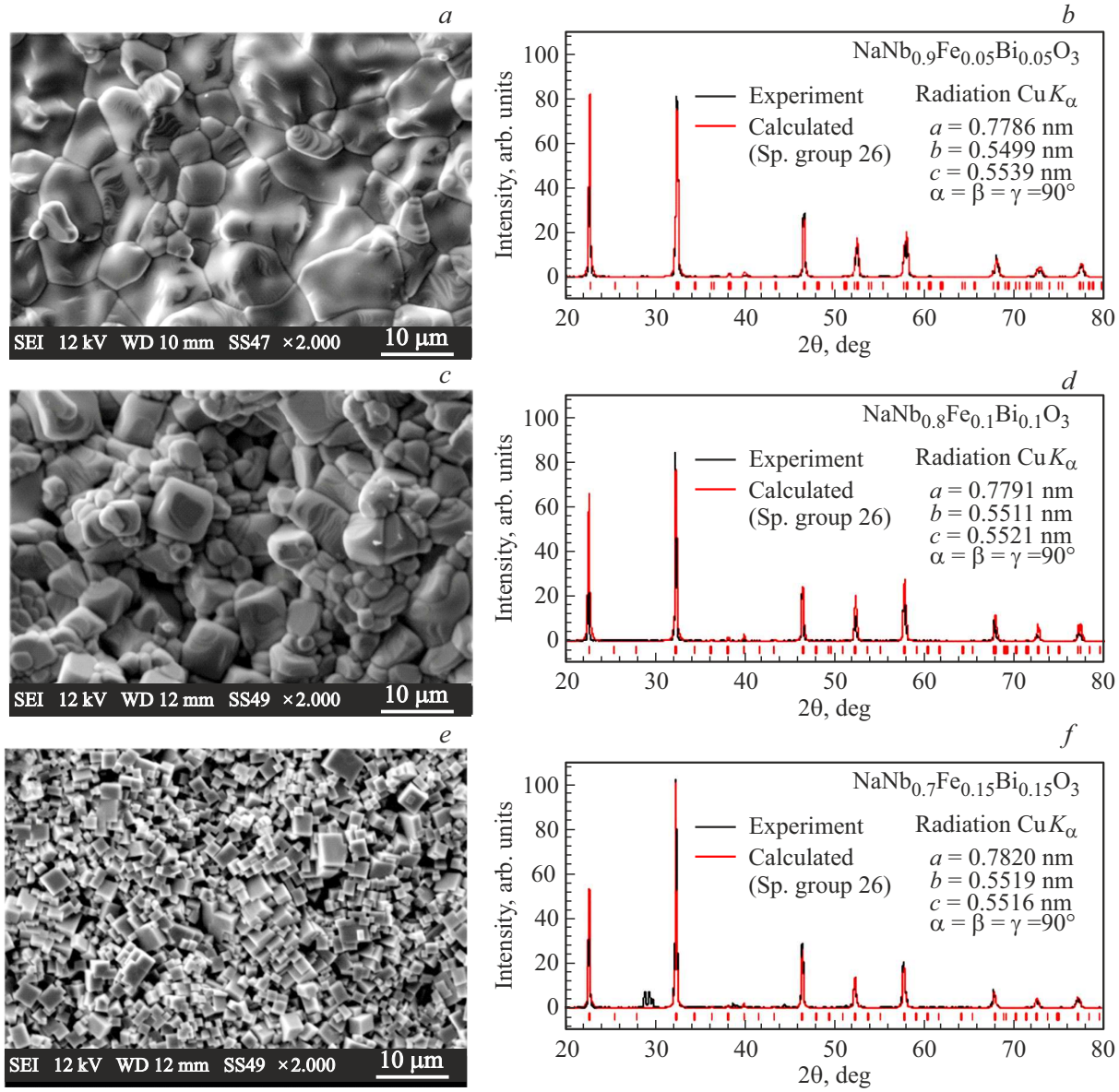

Figure 1. NNFB ceramic structure. SEM images of microstructure (a, c, e) and X-ray diffraction analysis data (b, d, f) of NNFB ceramic samples for $x = 0.1$ (a, b), $x = 0.2$ (c, d), $x = 0.3$ (e, f).

B-site lies in the niobium concentration range between 70 and 80 mol.%.

The frequency dependences of the complex dielectric permittivity for all samples are monotonically decreasing functions according to the results of dielectric spectroscopy. The dispersion diagrams are straight lines, and they form arcs of a semicircle in the high frequency region up to temperatures of 200–300 °C (depending on the composition) (Figure 2). The increase of both components of the complex permittivity with decreasing frequency is usually attributed to the influence of conductivity, which leads to charge separation and accumulation on structural inhomogeneities or in the near-electrode region [17]. Thus, the value of ε' increases at low frequencies and a linear dispersion due to Maxwell-Wagner polarization or electrode polarization is observed. For this reason the electrical modulus M is often used to determine the parameters of polarization mechanisms and analyze their behavior with temperature [18,19]. It is the inverse of the complex dielectric permittivity and is calculated by the formula [20]

$$M = M' + iM'' = \frac{\varepsilon'}{\varepsilon'^2 + \varepsilon''^2} + i\frac{\varepsilon''}{\varepsilon'^2 + \varepsilon''^2}, \qquad (1)$$

where ε' and ε'' are the real and imaginary parts of the complex dielectric permittivity, M' and M'' are the real and imaginary parts of the complex electric modulus. According to this definition, the values of the electric modulus at low frequencies $(M_0 = 1/\varepsilon_{(0)})$, where the dielectric permittivity $\varepsilon_{(0)}$ reaches very large values, are much less than 1, which allows the analysis of dielectric spectra.

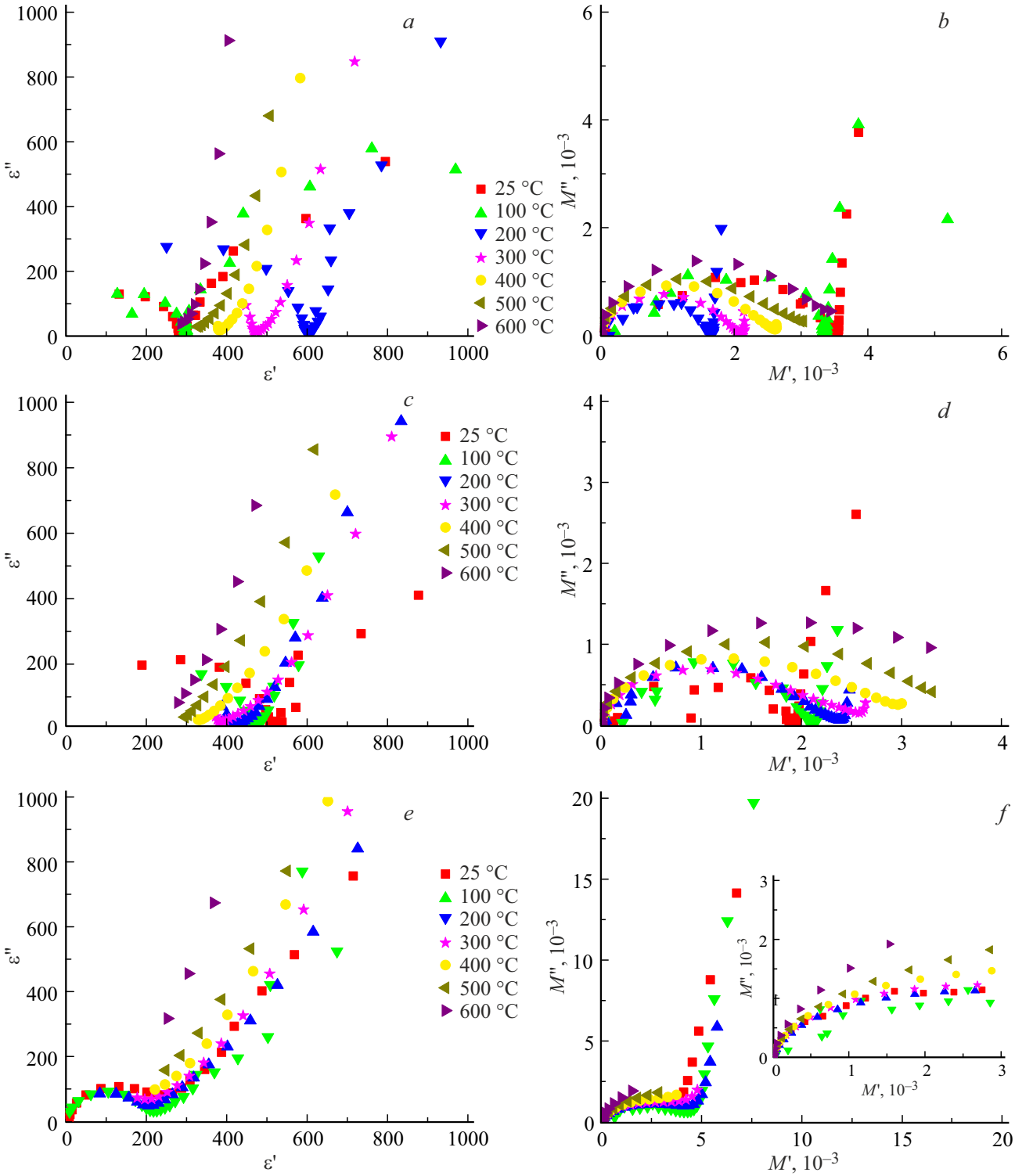

Figure 2. Diagrams of dispersion of complex dielectric permittivity (*a, c, e*) and electrical modulus (*b, d, f*) for ceramics $NN_{0.9}FB$ (*a, b*), $NN_{0.8}FB$ (*c, d*) and $NN_{0.7}FB$ (*e, f*).

Electrical modulus diagrams were constructed from the data obtained. As can be seen in Figure 2, the diagrams form two arcs of a semicircle at room temperature, indicating that two relaxation processes are taking place. When the temperature rises above 300 °C, the diagrams are transformed into one arc of a semicircle, the radius of which increases with increasing temperature, i. e., only one relaxation process is observed in the frequency range available for measurements. Due to the fact that the arcs of a semicircle are asymmetric and their centers are located

The most probable relaxation times for relaxation processes in NNFB ceramics

T, °C	$NN_{0.9}FB$		$NN_{0.8}FB$		$NN_{0.7}FB$	
	τ_1, s	τ_2, s	τ_1, s	τ_2, s	τ_1, s	τ_2, s
30	0.016	$2.3 \cdot 10^{-8}$	0.055	$2.3 \cdot 10^{-8}$	0.0045	$2.9 \cdot 10^{-7}$
100	0.016	$2.3 \cdot 10^{-8}$	0.032	$8.7 \cdot 10^{-9}$	0.0034	$3.4 \cdot 10^{-8}$
200	0.014	$2 \cdot 10^{-8}$	$7.3 \cdot 10^{-3}$	$4.5 \cdot 10^{-9}$	$2 \cdot 10^{-4}$	$1.9 \cdot 10^{-8}$
300	$3.9 \cdot 10^{-3}$	$4.2 \cdot 10^{-9}$	$1.6 \cdot 10^{-3}$	$3.5 \cdot 10^{-9}$	$2 \cdot 10^{-5}$	$4.6 \cdot 10^{-9}$
400	$3.6 \cdot 10^{-4}$	$3.4 \cdot 10^{-9}$	$1.2 \cdot 10^{-4}$	$3 \cdot 10^{-9}$	$9.8 \cdot 10^{-6}$	$2.5 \cdot 10^{-9}$
500	$4.6 \cdot 10^{-5}$	–	$1.1 \cdot 10^{-5}$	–	–	–
600	$7.8 \cdot 10^{-6}$	–	$2.1 \cdot 10^{-6}$	–	–	–
650	$2.3 \cdot 10^{-6}$	–	$1.5 \cdot 10^{-6}$	–	–	–

below the abscissa axis, the empirical Havriliak–Negami formula was used to analyze the $M''(M')$ diagrams [21]. The most probable relaxation time τ was determined from the frequency dependence of the imaginary part of the electric modulus, taking into account the offset of the relaxation frequency $(\omega_\tau = 1/\tau)$ relative to the frequency of the maximum $M''(\omega) - \omega_m$ due to the asymmetry of the relaxation time distribution function for this empirical formula [20]. The parameters were analyzed and selected using Mathcad software according to the Havriliak–Negami formula for two relaxation processes:

$$M = M_{\infty,2} + \frac{M_{0.1} - M_{\infty,1}}{(1 + (i\omega\tau_1)^{1-\lambda_1})^{\gamma_1}} + \frac{M_{0.2} - M_{\infty,2}}{(1 + (i\omega\tau_2)^{1-\lambda_2})^{\gamma_2}}, \quad (2)$$

where the parameters λ and γ characterize the diffusion and asymmetry of the relaxation time spectrum, respectively; M_0 and M_∞ are values of the real part of the electric modulus below $(\omega \ll \omega_m)$ and above $(\omega \gg \omega_m)$ the dispersion region for each relaxation process, respectively.

The calculated values of the relaxation times for all three samples support the assumption that the low-frequency relaxation process is most likely related to Maxwell-Wagner polarization (Table). This is characteristic of ceramic materials in which grain boundaries are the structural inhomogeneities that accumulate electric charge. In addition, for all samples, the relaxation time at low frequencies decreases both with increasing temperature and with increasing impurity concentration (in the temperature region above 200 °C). According to the formula of the compound $Na(Fe_{0.5}Bi_{0.5})_xNb_{1-x}O_{3-\delta}$, due to the difference in valence of the main ion (Nb^{5+}) in B-site and impurity ions (Fe^{3+}, Bi^{3+}), defects in the form of oxygen vacancies must be present in the ceramic structure. In such disordered materials, the existence of a hopping mechanism of conductivity, for example ionic or polaronic, is possible. In this case, the low-frequency maximum on the $M''(\omega)$ dependence observed in the region of linear dispersion of permittivity is called the „conductivity peak“ [18]. An increase in impurity concentration also, like an increase in temperature, leads to an increase in the number of defects and free charge carriers and hence an increase in conductivity. Thus, it can be concluded that the low-frequency dispersion of dielectric permittivity is attributable to ion or polaron hopping conductivity, which, due to the inhomogeneity of the structure of ceramic materials, leads to the accumulation of charge carriers on these inhomogeneities, which gives an additional contribution to the polarization of the sample.

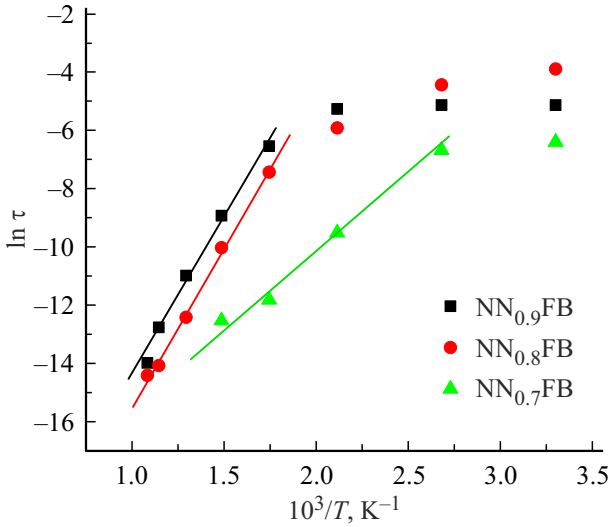

Figure 3. Temperature dependence of relaxation time for a low-frequency relaxation process in Arrhenius coordinates $\ln\tau\,(1/T)$.

As can be seen from Figure 2 and the table, the dielectric spectrum parameters of samples $NN_{0.9}FB$ and $NN_{0.8}FB$ have many similarities. In particular, the temperature dependence of the relaxation time has several regions close to each other in the characteristics of both compositions (Figure 3). For the exponential section in the temperature region above 300 °C, the activation energy E_a was determined from the Arrhenius equation for the relaxation time

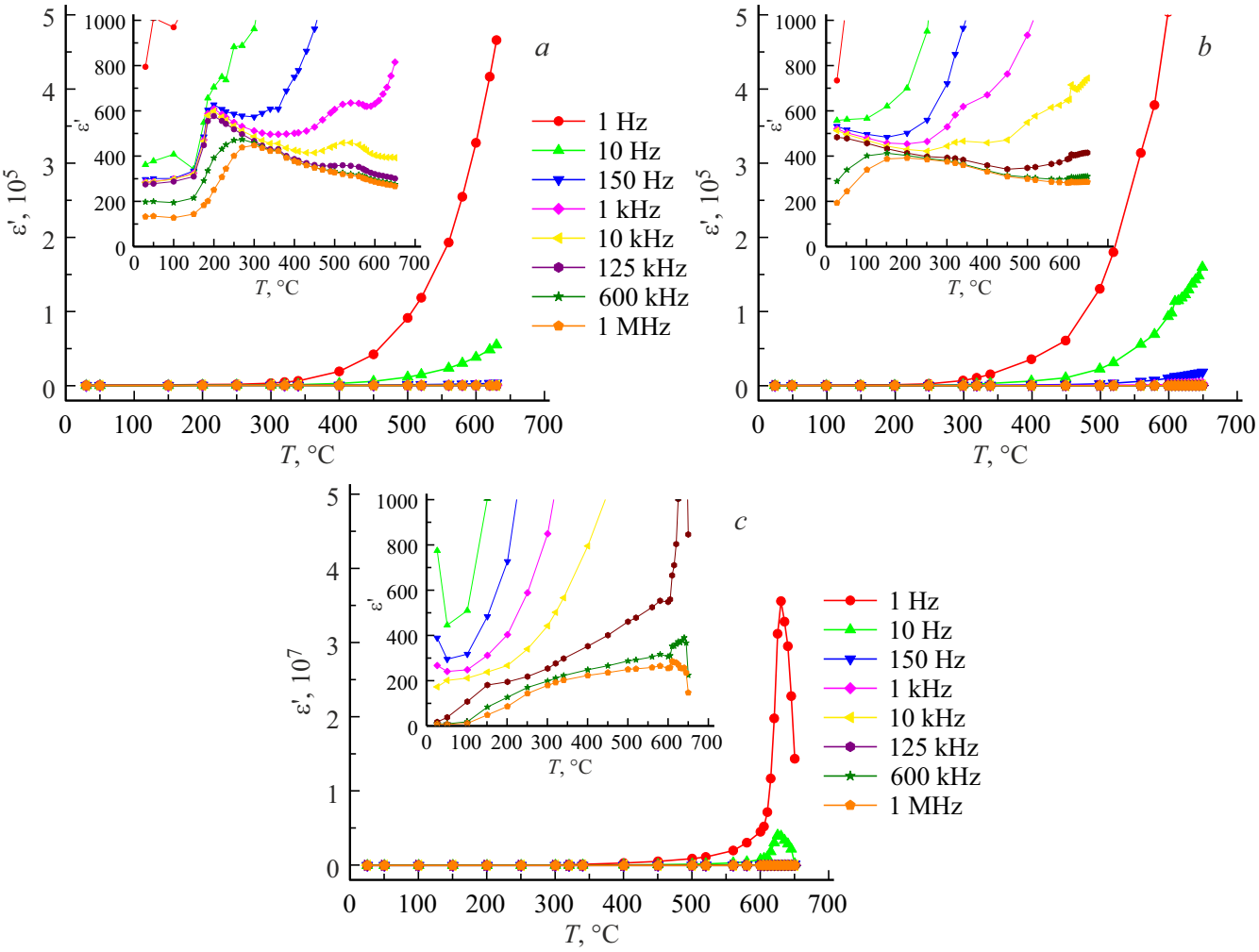

Figure 4. Temperature dependence of the real part of the dielectric permittivity for samples $NN_{0.9}FB$ (a), $NN_{0.8}FB$ (b), $NN_{0.7}FB$ (c).

$\tau = \tau_0 \exp(-E_a/kT)$, which was approximately 0.95 eV for both compositions. This value is smaller than the band gap in sodium niobate of 3.4–3.75 eV [11,22], but this energy may be sufficient for hopping conductivity.

A different picture is observed for the composition $NN_{0.7}FB$: the relaxation time of the low-frequency relaxation process is 1–2 order less than that of $NN_{0.9}FB$ and $NN_{0.8}FB$, and its rate of decrease with increasing temperature — is larger. Thus, this process is not observed at temperatures above 400°C. Its activation energy is 0.43 eV (Figure 3). The decrease in the value E_a can be explained by the fact that the increase in the concentration of point defects in the structure of this sample, compared to the other two, leads to a weakening of the bonding of ions in the crystal lattice, and thus a lowering of the potential barrier between the nodes of the lattice. Thus it can be said that the relaxation time of the low-frequency relaxation process as if „catches up“ with the relaxation time of the high-frequency process when the temperature changes. Which emphasizes the different nature of the charge carriers involved in these processes.

According to the relaxation time calculations τ_2, the high-frequency relaxation process in all the studied samples is due to thermal ionic polarization (Table), which is characteristic of ionic crystals.

From the results of measurements, the dependence of the real part of the complex dielectric permittivity on temperature was plotted. As can be seen in Figure 4, a, for the sample $NN_{0.9}FB$, a maximum of dielectric permittivity at frequency 1 kHz at 200 °C is observed in the plot $\varepsilon'(T)$, which shifts toward high temperatures (up to 300 °C) with increasing frequency of the measuring field at frequencies above 200 kHz (Figure 5, a). In this case, the phase transition region is a temperature range in which the maximum $\varepsilon'(T)$ is observed at different frequency of the measuring field increases and is approximately 300 °C at 1 MHz, i. e., phase transition is diffused. A second diffused maximum $\varepsilon'(T)$ is observed at 560 °C. It is worth noting that at frequencies below 150 Hz both maxima disappear and the dielectric permittivity increases monotonically with temperature. This is most likely due, as noted earlier, to the effect of conductivity on the complex dielectric permittivity, which leads to a distortion of the true dielectric response of the sample.

Phase transitions of pure sodium niobate, according to the literature [1,23,24], are observed at temperatures of 360, 430, 470, 520, 580, and 640 °C. It is interesting to note that sodium niobate ceramic samples doped separately with 10 mol.% of bismuth or iron, which we studied earlier, have maxima on the dependence $\varepsilon'(T)$ at temperatures 260 and 620 °C, respectively [25]. The Curie-Weiss law is satisfied above these temperatures, which is characteristic of ferroelectric phase transitions. Then it can be assumed that the doping of NN leads to a decrease in the temperature of phase transitions compared to un-doped ceramics (from 360 °C to 260 °C for systems with Bi, from 640 °C to 620 °C for systems with Fe), and depending on the type of impurity, the temperature of the main maximum changes (360 °C or 640 °C). In this case, both maxima are observed simultaneously when both impurities are doped, with the phase transition temperatures shifting to lower temperatures compared to separately doped compositions [25] (the low-temperature maximum shifts from 260 °C to 200 °C, and the high-temperature maximum shifts from 620 °C to 560 °C), and the low-temperature and high-temperature phase transition regions increase by a factor of 6 and 3, respectively.

These maxima are diffused in the sample $NN_{0.8}FB$ to such an extent that they become indistinguishable. The phase transition shifts to temperatures below room temperature at frequencies below 100 kHz. There are no maxima at low frequencies like in the case with the previous composition.

Ferroelectric with a diffused phase transition are characterized by the deviation of the relative permittivity in a sufficiently wide temperature range above T_m from the Curie-Weiss law and the fulfillment of the relation [26,27]:

$$\frac{1}{\varepsilon} - \frac{1}{\varepsilon_m} = \frac{(T - T_m)^n}{C}, \qquad (3)$$

where ε_m is the maximum value of the dielectric permittivity, T_m is the temperature of the maximum of the dielectric permittivity, C is the constant, and n represents the degree of phase transition diffused. An non-diffuse phase transition is observed at $n = 1$ and the Curie-Weiss law is fulfilled immediately after passing the temperature of the dielectric permittivity maximum on the dependence $\varepsilon(T)$, and $n = 2$ corresponds to the relaxor state. In the presence of relaxor properties, the maximum of the dielectric permittivity shifts to higher temperatures with increasing field frequency according to the Vogel-Fulcher law [28]:

$$\nu_m = \nu_0 \exp\left(\frac{E_a}{T_m - T_F}\right), \qquad (4)$$

where T_m is the temperature of the dielectric permittivity maximum at frequency ν_m, E_a is the activation energy, T_F is the Vogel-Fulcher-Tamman temperature (temperature of „freezing“ of dipoles). The analysis of the main low-temperature phase transition has shown that the studied compositions $NN_{0.9}FB$ and $NN_{0.8}FB$ have values of the

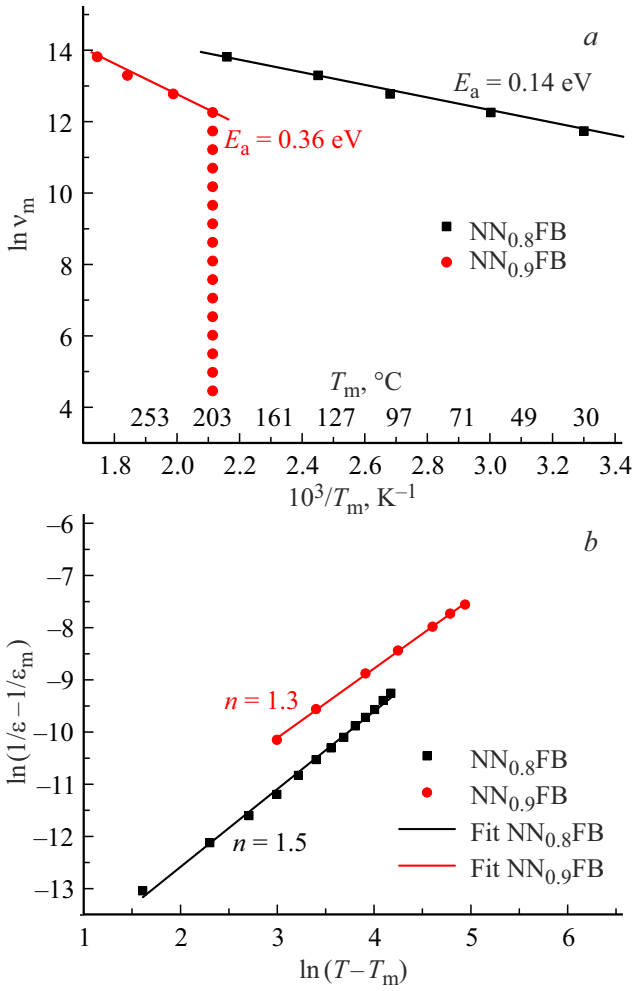

Figure 5. (*a*) The dependence of the frequency of the dielectric permittivity maximum on temperature in Arrhenius coordinates $\ln \nu_m(1/T)$; (*b*) charts of the dependence of $\ln(1/\varepsilon - 1/\varepsilon_m)$ as a function of $\ln(T - T_m)$ at 200 kHz for samples $NN_{0.8}FB$ and $NN_{0.9}FB$.

index n, characterizing the degree of phase transition diffusion, lying in the range from 1 to 2 (Figure 5, *b*). In addition, the relationship between frequency and temperature of the maximum of the dielectric permittivity is described by Arrhenius's law (5), not by the expression (4). Consequently, these compositions are materials with a diffused phase transition but do not exhibit relaxor properties. According to the formula

$$\nu_m = \nu_0 \exp\left(\frac{E_a}{kT_m}\right) \qquad (5)$$

the energy E_a of the processes leading to a shift with frequency of the position ε_m on the temperature dependence $\varepsilon'(T)$ was determined. As follows from Figure 5, *a*, the activation energy of this process decreases with increasing impurity concentration. This explains the increase in the phase transition region: it is 100 °C (from 200 to 300 °C) for the sample $NN_{0.9}FB$, and more than 160 °C (from 30 or less to 190 °C) for sample $NN_{0.8}FB$.

When the impurity concentration is increased up to 30 mol.%, the temperature dependence of the dielectric permittivity changes. Specifically, the maxima observed in other compositions are absent, the dielectric permittivity increases with increasing temperature, and a maximum $\varepsilon'(T)$ appears at 625 °C. This maximum shifts to the high temperature region with increasing frequency, but the broadening of the peak is very small. It is noteworthy that the value of ε' for the sample $NN_{0.7}FB$ in the low temperature and high frequency region is two orders of magnitude smaller than for the other compositions. The comparison of the values of relaxation times for the high-frequency process (table) of samples $NN_{0.7}FB$ and $NN_{0.8}FB$, $NN_{0.9}FB$ shows that the thermal ion polarization in this composition begins to lag behind the field in the indicated frequency and temperature ranges at lower frequencies than in the other compositions. When the polarization mechanism is „off" (at frequencies above the relaxation maximum), it makes no contribution to the polarization of the sample, leading to a decrease in the dielectric permittivity.

4. Conclusion

The conducted studies of the structure and dielectric properties of sodium niobate ceramics doped with Fe and Bi at *B*-site allow making a conclusion that the concentration of impurities changes the shape and grain size of NN ceramics without changing the crystallographic symmetry of the lattice. Minor amounts of unidentified second phase appear in the samples with impurity concentrations greater than 20 mol.%. Two relaxation processes are observed in all compositions: a low-frequency one due to electrical conductivity and a high-frequency one related to thermal ion polarization. The relaxation times of these processes decrease as the temperature increases. The pattern of phase transitions determined from the maxima of the temperature dependence of the dielectric permittivity depends on the impurity concentration. Two diffused phase transitions ($n = 1.3$ and 1.5, respectively) are observed at frequencies above 150 Hz in samples $NN_{0.9}FB$ and $NN_{0.8}FB$, the temperature of these phase transitions decreases with increasing impurity concentration. There is an additional contribution to the dielectric permittivity below 150 Hz due to the accumulation of charges involved in conductivity on the structure heterogeneities that masks all extrema on the dependence $\varepsilon'(T)$.

Funding

This study was carried out under the state assignment for scientific activity № 0817-2023-0006 with the use of resources of the Research Laboratory of Electron Microscopy and Magnetic Materials of the Center for Collective Use of „Tver State University".

Conflict of interest

The authors declare no conflict of interest.

References

[1] H.D. Megaw. Ferroelectrics **7**, *1*, 87 (1974).
[2] L.A. Reznichenko, L.A. Shilkina, E.S. Gagarina, I.P. Raevskii, E.A. Dul'kin, E.M. Kuznetsova, V.V. Akhnazarova. Crystallogr. Rep. **48**, *3*, 448 (2003).
[3] R.A. Shakhovoy, S.I. Raevskaya, L.A. Shakhovaya, D.V. Suzdalev, I.P. Raevski, Yu.I. Yuzyuk, A.F. Semenchev, M. El Marssi. J. Raman Spectrosc. **43**, 1141 (2012).
[4] L.E. Cross, B.J. Nicholson. Philos. Mag. **46**, *376*, 453 (1955).
[5] J.G. Wu, D.Q. Xiao, J.G. Zhu. Chem. Rev. **115**, *7*, 2559 (2015).
[6] Yu.I. Yuzyuk, P. Simon, E. Gagarina, L. Hennet, D. Thiaudière, V.I. Torgashev, S.I. Raevskaya, I.P. Raevskii, L.A. Reznitchenko, J.L. Sauvajol. J. Phys.: Condensed Matter **17**, *33*, 4977 (2005).
[7] J. Koruza, P. Groszewicz, H. Breitzke, G. Buntkowsky, T. Rojac, B. Malič. Acta Materialia **126**, 77 (2017).
[8] J. Koruza, J. Tellier, B. Malič, V. Bobnar, M. Kosec. J. Appl. Phys. **108**, 113509 (2010).
[9] Y. Fan, Z. Zhou, R. Liang, M. Zhou, X. Dong. J. European Cer. Soc. **39**, *15*, 4712 (2019).
[10] D. Kaneria, D. Yadav, U. Jamwal, S.K. Mittal, K.L. Yadav. J. Power Sources **613**, 234948 (2024).
[11] B.K. Yun, Y.K. Park, P.G. Kang, J.H. Jung, N. Lee, W. Jo, H. Shin, S. Yoon. Mat. Sci. and Engin. B **182**, 81 (2014).
[12] Tania, S. Chaudhary, S. Jindal. Interactions **245**, 143 (2024).
[13] L. Lu, L. Li, P. Ren, X. Che, G. Zhao. Ceram. Intern. **48**, 32073 (2022).
[14] E.V. Barabanova, A.I. Ivanova, O.V. Malyshkina, E.S. Tesnikova, M.S. Vahrushev. Ferroelectrics **559**, *1*, 22 (2020).
[15] P. Vlazan, M. Poienar, I. Malaescu, C.N. Marin, C. Casut, P. Sfirloaga Chem. Phys. **579**, 112203 (2024).
[16] P. Villars (Chief Editor), pauling file in: Inorganic Solid Phases, SpringerMaterials (online database), Springer, Heidelberg (2016).
[17] A.K. Jonscher. J. mater. Sci. **26**, 1618 (1991).
[18] J.J. Fontanella, J.J. Wilson, M.K. Smith, M.C. Wintersgill, C.S. Coughlin, P. Mazaud, S.G. Greenbaum, R.L. Siddon. Solid State Ionics **50**, 259 (1992).
[19] N.G. McCrum, B.E. Read, and G. Williams. Anelastic and dielectric effects in polymeric solids. John Wiley and Sons Ltd., London. (1967). 617 p.
[20] A.K. Jonscher. Dielectric relaxation in solids. Chelsea Dielectrics Press., London. (1983). 380 p.
[21] S. Havriliak, S. Negami. J. Polym. sci. C. **14**, 99 (1966).
[22] P. Vlazan, S.F. Rus, M. Poienar, P. Sfirloaga. Mat. Sci. Semicon. Proc. **102**, 104602 (2019).
[23] Y. Saito, H. Takao, T. Tani, T. Nonoyama, K. Takatori, T. Homma, T. Nagaya, M. Nakamura. Nature **432**, 84 (2004).
[24] E.A. Wood. Acta Cryst. **4**, *4*, 353 (1951).
[25] N.M. Ospelnikov. E.V. Barabanova. Izvestiya RAN. Seriya fizicheskaya **87**, *4*, 546 (2023). (in Russian).
[26] K. Uchino, S. Nomura. Ferroelectrics **44**, *1*, 55 (1982).
[27] H. Du, W. Zhou, F. Luo. et al. J. Appl. Phys. **105**, 12 (2009).
[28] L.S. Garca-Coln, L.F. del Castillo, P. Goldstein. Phys. Rev. B **41**, 4785 (1990).

Translated by A.Akhtyamov